

Temperature induced single domain–vortex state transition in sub-100 nm Fe nanodots

Randy K. Dumas and Kai Liu^{a)}

Physics Department, University of California, Davis, California 95616, USA

Chang-Peng Li, Igor V. Roshchin,^{b)} and Ivan K. Schuller

Physics Department, University of California-San Diego, La Jolla, California 92093, USA

(Received 30 September 2007; accepted 19 October 2007; published online 12 November 2007)

Magnetization reversal in nanomagnets via a vortex state, although often investigated at the remanent state, may not necessarily display a zero remanence or a highly pinched hysteresis loop. In contrast, the irreversible nucleation/annihilation events are clear indications of a vortex state. In this work, temperature induced single domain–vortex state transition has been investigated in 67 nm Fe nanodots using a first-order reversal curve (FORC) technique. The two phase coexistence is manifested as different features in the FORC distribution. At lower temperatures, it becomes harder to nucleate and annihilate vortices and the amount of single domain dots increases. © 2007 American Institute of Physics. [DOI: 10.1063/1.2807276]

Magnetic nanoelements have been a focus research area due to their interesting fundamental properties and potential in ultrahigh density magnetic recording and memory applications.^{1–4} It is known that well above the domain wall width, in micron and submicron sized patterns, magnetization reversal often occurs via a vortex state (VS).^{5–8} As the nanoelement dimension approaches the exchange length, single domain (SD) static states are energetically more favorable. There have been extensive theoretical and experimental studies on SD-VS phase diagrams as a function of nanomagnet dimensions.^{6,8–10} Typically, e.g., in isotropic circular dots, the VS evolution from positive saturation starts with an abrupt magnetization drop at a positive nucleation field, followed by a flux closure state with zero remanence and finally the vortex annihilation at a negative field.⁶ Observation of the VS at remanence using magnetic microscopy⁵ has indeed become a common practice. However, ultrasmall nanodots or nanorings may exhibit a SD remanent state, due to the more prominent role of boundaries, even though the magnetization reversal involves a VS.^{4,11} Similarly, when a strong anisotropy is present, such as in elliptical or rectangular dots with a well defined shape anisotropy, the minimal demagnetization field along the magnetic easy axis may shift the vortex nucleation field to negative values, leading to a SD state at remanence.^{12,13} The hysteresis loops, particularly those of a collection of nanomagnets, no longer bear the characteristic highly “pinched” shape with a zero remanence. Additionally, at such small dimensions, temperature becomes increasingly more important in influencing the nanomagnet reversal behaviors. Recent studies have shown that near the SD-VS phase boundary, both phases can be stabilized and conversion from one to the other can be triggered by thermal activation or magnetic field cycling.^{8,10} Therefore, it is not always reliable to use the nanomagnet remanent magnetic configuration or the shape of the hysteresis loop to determine the presence of VS.¹⁴

On the other hand, the irreversible events associated with vortex nucleation and annihilation are clear signatures of VS. They can be used to track the nanomagnets that reverse via VS, regardless whether the remanent state is VS or not. We have recently shown in sub-100 nm Fe nanodots, using a first-order reversal curve (FORC) technique,^{15–18} that SD and VS indeed have drastically different “fingerprints” due to their respective irreversible magnetization switching mechanisms.¹⁹ In this letter, we quantitatively investigate the temperature dependent SD-VS transition in arrays of 67 nm diameter Fe nanodots. The FORC diagrams reveal not only qualitatively the presence of both SD and VS phases but also quantitatively the amount of nanodots that reverse via each mode, or the phase fractions. At lower temperatures, the SD phase fraction increases while the vortices become harder to nucleate and annihilate.

High density arrays of Fe nanodots ($\sim 10^{10}/\text{cm}^2$) have been fabricated over macroscopic areas ($\sim 1 \text{ cm}^2$) using a nanoporous alumina shadow mask technique in conjunction with electron beam evaporation.^{20,21} The nanodots have been grown on silicon substrates with a diameter of $67 \pm 13 \text{ nm}$ and a thickness of 20 nm, similar to those reported earlier.¹⁹ The Fe dots thus made are polycrystalline, capped with a Ag layer. Because the nanodot center-to-center spacing is roughly twice its diameter, dipolar interactions are negligible.¹¹

Magnetic properties have been measured using a Princeton Measurements Corp. vibrating sample magnetometer with a liquid helium flow cryostat. The applied field is in the plane of the nanodots. The sample has been cut down to $\sim 3 \times 3 \text{ mm}^2$ pieces, each containing $\sim 10^9$ Fe nanodots. The FORC technique has been employed to study details of the magnetization reversal. After saturation, the magnetization M is measured starting from a reversal field H_R back to positive saturation, tracing out a FORC. A family of FORC's is measured at different H_R , with equal field spacing. The FORC distribution is defined as^{15–17,19}

$$\rho(H_R, H) \equiv -\frac{1}{2} \frac{\partial^2 M(H_R, H)/M_s}{\partial H_R \partial H}, \quad (1)$$

which eliminates the purely reversible components of the

^{a)}Author to whom correspondence should be addressed. Electronic mail: kailiu@ucdavis.edu

^{b)}Also at Physics Department, Texas A&M University.

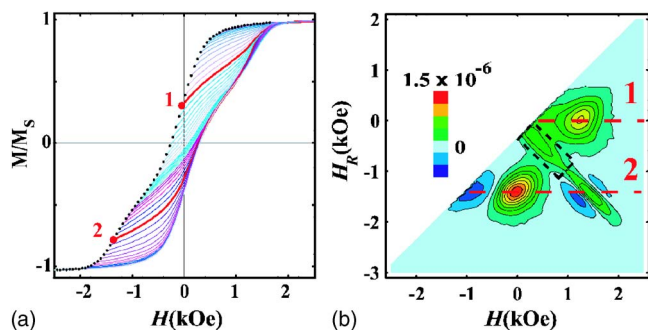


FIG. 1. (Color online) (a) A family of FORC's for the 67 nm Fe nanodots at 300 K, whose starting points are represented by black dots. (b) The corresponding FORC distribution as a contour plot against applied field H and reversal field H_R . The two red FORC's in (a) correspond to line scans 1 and 2 in (b). The dotted black box in (b) highlights a residual FORC feature due to single domain nanodots.

magnetization. Thus, any nonzero ρ corresponds to *irreversible* switching processes.^{17,19} The FORC distribution can also be represented in (H_C, H_B) coordinates, where H_C is the local coercive field and H_B is the interaction field, through a rotation of the coordinate system defined by $H_B = (H + H_R)/2$ and $H_C = (H - H_R)/2$.

In a recent study we investigated the room temperature magnetization reversal behaviors of Fe nanodots in the size range of 52–67 nm.¹⁹ Despite only subtle differences in the major magnetic hysteresis loops, the 52 and 67 nm nanodots respectively exhibit SD and mostly VS behavior. The VS is separately confirmed by polarized neutron reflectivity measurements on similarly prepared 65 nm Fe dots.²² For the present 67 nm Fe nanodots, the family of FORC's at 300 K is shown in Fig. 1(a), where the black dots mark the starting points for each FORC. The major hysteresis loop, traced by the outer boundary of the FORC's, shows a slight pinch near zero field. The corresponding FORC distribution ρ , plotted as a contour plot in the (H, H_R) coordinate system, is shown in Fig. 1(b). The degree of irreversibility along a given FORC [Fig. 1(a)] is represented by the value of ρ along a horizontal line scan at reversal field H_R in the FORC distribution [Fig. 1(b)]. Because VS nucleation and annihilation events are highly irreversible processes, their FORC “fingerprints” can be easily interpreted in the (H, H_R) coordinates. Along line scan 1 ($H_R = -20$ Oe), vortices have already nucleated in most of the nanodots. With increasing field H , ρ becomes nonzero, peaks at $H = 1220$ Oe, and returns to zero near positive saturation. This feature corresponds to the annihilation of the vortices in the nanodots. Line scan 2 starts at $H_R = -1370$ Oe, where majority of the nanodots have been negatively saturated. As H is increased, a first maximum in ρ is seen at $H = 20$ Oe, corresponding to the nucleation of vortices within the nanodots. At $20 \text{ Oe} < H < 1370 \text{ Oe}$, ρ is very small, indicating the highly reversible motion of the vortices through the nanodots. A second ρ maximum is found at $H = 1370$ Oe, as the vortices are annihilated. This is again followed by reversible behavior near positive saturation. The locations of these three peaks in the FORC distribution directly map out the VS nucleation and annihilation fields, as confirmed by micromagnetic simulations.¹⁹ The peaks in Fig. 1(b) are rather broad, which is a manifestation of variations in VS nucleation and annihilation fields among the 10^9 nanodots in the sample. Note that there is yet another ridge in the FORC distribution, highlighted by the dotted box in

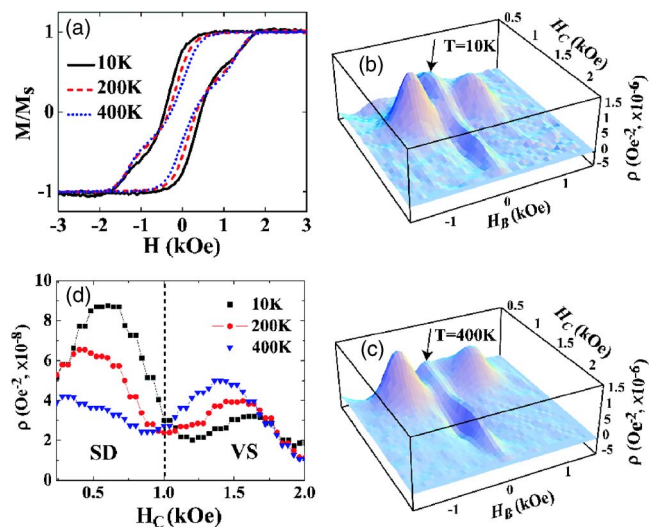


FIG. 2. (Color online) (a) Representative major hysteresis loops at 10, 200, and 400 K, and three-dimensional FORC distributions at (b) 10 K and (c) 400 K. The black arrow in (b) and (c) indicates a feature in the FORC distribution due to the single domain phase. A cross-sectional view of the FORC distribution along the local coercivity axis ($H_B = 0$) is shown in (d).

Fig. 1(b). This feature corresponds to a residual SD phase, similar to that seen in 52 nm noninteracting SD Fe nanodots.¹⁹

Furthermore, the integration $I_{\text{Irrev}} = \int \rho(H_R, H) dH_R dH = \int \rho(H_B, H_C) dH_B dH_C$ captures the total amount of irreversible magnetic switching in a sample.¹⁸ Thus, it can be used to quantitatively determine the amount of magnetic phases.^{19,23} By selectively integrating the normalized FORC distribution over the boxed region in Fig. 1(b), compared to that over the entire FORC diagram, we find a SD phase fraction of 16%; i.e., roughly 16% of the 67 nm dots remain in the SD phase during reversal while the rest of the dots reverse via a VS.

The magnetization reversal behaviors have been investigated at different temperatures. Shown in Fig. 2(a) are three representative major hysteresis loops at 10, 200, and 400 K. At lower temperatures, the slight loop pinch near zero field becomes less apparent as the loop widens. From 400 to 10 K, the coercivity increases from 280 to 440 Oe while the normalized remanence M_r/M_s increases from 36% to 72%. The much larger remanence at 10 K is not necessarily an indication of a predominantly SD phase; a shift of the VS nucleation field toward more negative fields could also increase M_r/M_s . These contributions, while convoluted in the major hysteresis loop, can be distinguished clearly in the FORC distributions.

Shown in Figs. 2(b) and 2(c) are FORC distributions in the (H_B, H_C) coordinate system at 10 and 400 K, respectively. The black arrow indicates a ridge in the FORC distribution due to the SD phase, as highlighted by the dotted box in Fig. 1(b). The other three outstanding features correspond to the VS nucleation/annihilation fields discussed above. The qualitatively similar FORC patterns indicate that VS still dominates within the temperature range. On the other hand, the SD ridge is more prominent at 10 K, suggesting an increase of SD phase fraction. This trend is more apparent in the cross-sectional view of the FORC distribution along the H_C axis ($H_B = 0$), shown in Fig. 2(d). The first peak at $H_C < 1$ kOe corresponds to the SD phase while the second one at $H_C > 1$ kOe is related to the VS, caused by the annihilation

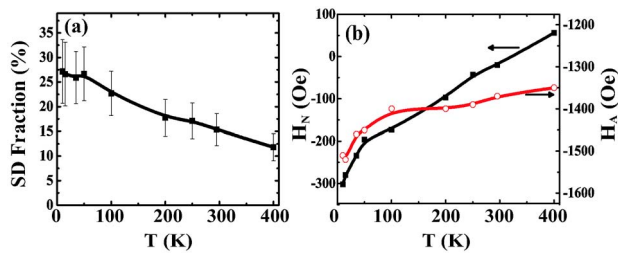


FIG. 3. (Color online) (a) Percentage of the nanodots that are single domain at a given temperature. (b) Temperature dependence of the nucleation (solid squares) and annihilation (open circles) fields of the vortex phase, determined from peak positions in the FORC distribution. Solid lines are guides to the eye.

of vortices when reversing from near negative saturation. As temperature is decreased, the SD feature grows at the expense of the VS peak, indicating a larger fraction of SD dots at lower temperatures. As discussed earlier, a quantitative estimate of the SD phase fraction can be obtained by selectively integrating the SD portion of the normalized FORC distribution. Figure 3(a) shows that the SD phase fraction indeed increases from 12% at 400 K to 27% at 10 K.

The FORC distributions also contain quantitative information about the VS nucleation and annihilation fields, which cannot be obtained from the ensemble-averaged major hysteresis loops. Considering a reversal from positive saturation, the VS nucleation field H_N and annihilation field H_A are the reversal fields H_R for line scans 1 and 2 in Fig. 1(b), respectively.¹⁹ With decreasing temperature, both H_N and H_A shift to more negative values, as shown in Fig. 3(b). At lower temperatures, it not only becomes more difficult to nucleate vortices within the dots but it also takes a larger field to annihilate the vortices from the dots. This trend is consistent with the thermally activated nature of VS nucleation annihilation.²⁴ Those dots with sizes near the SD-VS phase boundary are more likely to stay in the SD state at low temperatures, but reverse at elevated temperatures through thermally assisted vortex nucleation and motion. Hence, the SD phase fraction is larger at lower temperatures. The larger remanence seen at 10 K is due to both the increase in SD phase fraction and the shift of the vortex nucleation field.

In summary, we have investigated the SD-VS transition in arrays of 67 nm Fe nanodots at different temperatures using the FORC technique. Majority of the nanodots reverse via a vortex state. The irreversible vortex nucleation/annihilation events lead to distinct features in the FORC distribution, independent of the nanodot remanent magnetic configuration. Small fraction of the nanodots are in the SD

phase, with a characteristically different FORC distribution. At lower temperatures, the lack of thermal activation makes it harder to nucleate and subsequently annihilate vortices. As a result, those nanodots closest to the VS-SD phase boundary are unable to reverse via VS and become SD entities.

This work has been supported by ACS (PRF-43637-AC10), AFOSR, and the Alfred P. Sloan Foundation. We thank J. E. Davies, J. Olamit, M. Winklhofer, C. R. Pike, H. G. Katzgraber, R. T. Scalettar, G. T. Zimányi, and K. L. Verosub for helpful discussions.

- ¹C. Ross, *Annu. Rev. Mater. Res.* **31**, 203 (2001).
- ²J. I. Martin, J. Nogues, K. Liu, J. L. Vicent, and I. K. Schuller, *J. Magn. Magn. Mater.* **256**, 449 (2003).
- ³S. D. Bader, *Rev. Mod. Phys.* **78**, 1 (2006).
- ⁴C. L. Chien, F. Q. Zhu, and J. G. Zhu, *Phys. Today* **60**(6), 40 (2007).
- ⁵T. Shinjo, T. Okuno, R. Hassdorf, K. Shigeto, and T. Ono, *Science* **289**, 930 (2000).
- ⁶R. Cowburn, D. Koltsov, A. Adeyeye, M. Welland, and D. Tricker, *Phys. Rev. Lett.* **83**, 1042 (1999).
- ⁷K. Guslienko, V. Novosad, Y. Otani, H. Shima, and K. Fukamichi, *Phys. Rev. B* **65**, 024414 (2002).
- ⁸H. F. Ding, A. K. Schmid, D. Q. Li, K. Y. Guslienko, and S. D. Bader, *Phys. Rev. Lett.* **94**, 157202 (2005).
- ⁹H. Hoffmann and F. Steinbauer, *J. Appl. Phys.* **92**, 5463 (2002).
- ¹⁰Y. Li, P. Xiong, S. von Molnár, Y. Ohno, and H. Ohno, *Phys. Rev. B* **71**, 214425 (2005).
- ¹¹J. Mejia-Lopez, D. Altbir, A. H. Romero, X. Battle, I. V. Roshchin, C.-P. Li, and I. K. Schuller, *J. Appl. Phys.* **100**, 104319 (2006).
- ¹²A. Fernandez, M. R. Gibbons, M. A. Wall, and C. J. Cerjan, *J. Magn. Magn. Mater.* **190**, 71 (1998).
- ¹³J. Shi, J. Li, and S. Tehrani, *J. Appl. Phys.* **91**, 7458 (2002).
- ¹⁴V. Rose, X. M. Cheng, D. J. Keavney, J. W. Freeland, K. S. Buchanan, B. Ilic, and V. Metlushko, *Appl. Phys. Lett.* **91**, 132501 (2007).
- ¹⁵C. Pike and A. Fernandez, *J. Appl. Phys.* **85**, 6668 (1999).
- ¹⁶H. G. Katzgraber, F. Pazmandi, C. R. Pike, K. Liu, R. T. Scalettar, K. L. Verosub, and G. T. Zimanyi, *Phys. Rev. Lett.* **89**, 257202 (2002).
- ¹⁷J. E. Davies, O. Hellwig, E. E. Fullerton, G. Denbeaux, J. B. Kortright, and K. Liu, *Phys. Rev. B* **70**, 224434 (2004).
- ¹⁸J. Olamit, K. Liu, Z. P. Li, and I. K. Schuller, *Appl. Phys. Lett.* **90**, 032510 (2007).
- ¹⁹R. K. Dumas, C.-P. Li, I. V. Roshchin, I. K. Schuller, and K. Liu, *Phys. Rev. B* **75**, 134405 (2007).
- ²⁰K. Liu, J. Nogues, C. Leighton, H. Masuda, K. Nishio, I. V. Roshchin, and I. K. Schuller, *Appl. Phys. Lett.* **81**, 4434 (2002).
- ²¹C.-P. Li, I. V. Roshchin, X. Battle, M. Viret, F. Ott, and I. K. Schuller, *J. Appl. Phys.* **100**, 074318 (2006).
- ²²I. V. Roshchin, C.-P. Li, H. Suhl, X. Battle, J. Mejia-Lopez, D. Altbir, A. H. Romero, S. Roy, S. K. Sinha, M. Fitzimmons, and I. K. Schuller (unpublished).
- ²³J. E. Davies, J. Wu, C. Leighton, and K. Liu, *Phys. Rev. B* **72**, 134419 (2005).
- ²⁴H. Shima, V. Novosad, Y. Otani, K. Fukamichi, N. Kikuchi, O. Kitakamai, and Y. Shimada, *J. Appl. Phys.* **92**, 1473 (2002).